The effect of Al substitution for Ni on the structure and electrochemical properties of AB$_3$-type La$_2$Mg(Ni$_{1-x}$Al$_x$)$_9$ (x = 0–0.05) alloys

B. Liao[a], Y.Q. Lei[a,*], L.X. Chen[a], G.L. Lu[b], H.G. Pan[a], Q.D. Wang[a]

[a] *Department of Materials Science and Engineering, Zhejiang University, Hangzhou 310027, PR China*
[b] *Central Laboratory, Zhejiang University, Hangzhou 310027, PR China*

Abstract

The effect of replacing part of Ni by Al in La$_2$MgNi$_9$ alloy on the structure and electrochemical properties of the thus formed La$_2$Mg(Ni$_{1-x}$Al$_x$)$_9$ (x = 0–0.05) quaternary alloys was investigated. All alloys consisted of a main phase with hexagonal PuNi$_3$-type structure and a small quantity of an impurity phase (La$_2$Ni$_7$). The increase of Al content in the alloys leads to an increase in both the cell volume and the hydride stability, and leads to a noticeable decrease in cell volume expansion rate ($\Delta V/V$) on hydriding. The increase of Al content leads to some decrease in both the discharge capacity and the high-rate dischargeability (HRD) but leads to a significant improvement in cycling stability of the alloys. The decrease of HRD of the alloys is ascribed to the decrease of electrocatalytic activity for the hydrogen electrode reaction and the lower diffusion rate of hydrogen in the bulk of the alloys, while the improvement in cycling stability is mainly attributed to the decrease of V_H of the hydride phase.
© 2005 Elsevier B.V. All rights reserved.

Keywords: Hydrogen storage alloy; Al substitution; PuNi$_3$-type structure; Electrochemical property; Cell volume expansion on hydriding

1. Introduction

Recently, based on the discovery of a new type of R–Mg–Ni (R = rare earth, Ca, Y) system alloys with PuNi$_3$ type structure and a high hydrogen storage capacity [1–3], some of the R–Mg–Ni based alloys have been found to have a much higher discharge capacity (356–410 mAh/g) than that of AB$_5$-type alloys [2,3]. In our previous papers, we also reported that the La$_2$MgNi$_9$ ternary alloy with PuNi$_3$ type structure showed a high discharge capacity around 400 mAh/g [4,5]. In view of their higher electro-chemical capacities and low costs, the La–Mg–Ni based alloys have been considered as new candidates for the negative electrode materials of Ni/MH batteries. However, for commercial applications the rather poor cycling stability of the La–Mg–Ni system alloys has to be further improved. It is well known that element substitution is one of the effective methods for improving the overall properties of

the hydrogen storage alloys [6,7]. In our previous study on the La$_2$Mg(Ni$_{0.95}$M$_{0.05}$)$_9$ (M = Co, Al, Cu, Fe, Mn) alloys, we also found that the partial substitution of Al for Ni in La$_2$MgNi$_9$ alloy greatly improved the cycling stability of the alloy, but it led to a large reduction in both discharge capacity and the high-rate dischargeability [8]. It is expected that an optimized amount of Al substitution for Ni in La$_2$MgNi$_9$ alloy may lead to an alloy with high discharge capacity and good cycling stability, and hence is worthy to be determined.

In the present work, La$_2$Mg(Ni$_{1-x}$Al$_x$)$_9$ (x = 0.01–0.05) alloy samples were prepared. The effect of Al substitution for Ni on the crystal structure and the electrochemical properties of the alloys with different Al content were systematically investigated.

2. Experimental details

La$_2$Mg(Ni$_{1-x}$Al$_x$)$_9$ (x = 0.01–0.05) alloy samples were prepared by sintering the mixtures of LaNi$_{3-4.5x}$Al$_{4.5x}$,

MgNi$_2$ and Ni powders as described in previous papers [4,5]. These samples were mechanically pulverized to 300 mesh. The crystal structure of the alloys and their hydride samples was characterized with XRD analysis on a Rigaku D/Max 2550/PC X-ray diffractometer with Cu Kα radiation [5]. For electrochemical test, pellet type alloy electrodes ($d = 10$ mm) were prepared by cold pressing the mixtures of the alloy powder and the carbonyl nickel powder in the weight ratio of 1:3, and the electrochemical tests were conducted at 25 °C in a conventional three-compartments electrochemical cell as reported in our previous papers [4,5]. The discharge capacity was determined galvanostatically by using an automatic charge/discharge unit. Each electrode was charged at 200 mA/g for 2.5 h followed by a 10 min rest, and then discharged at 50 mA/g to the cutoff potential of −0.6 V versus Hg/HgO. For cycling tests, the activated electrode was charged each time at 200 mA/g for 2.5 h and discharged at 100 mA/g to −0.6 V versus Hg/HgO, and the discharge capacity at 50 mA/g was measured after every 10 cycles. In evaluating the rate capacity, discharge capacity of the alloy electrode at 800 mA/g was measured. The high-rate dischargeability (HRD$_{800}$), defined as $100 \times C_{800}/(C_{800} + C_{50})$, was determined from the ratio of the discharge capacity measured at 800 mA/g (C_{800}) to the total capacity defined as the sum of C_{800} and C_{50}, which was the additional capacity measured subsequently at 50 mA/g after C_{800} was measured. The electrochemical pressure–composition (P–C) desorption isotherms of the alloy at 25 °C were determined as reported in a previous paper [4]. The exchange current density I_0 of alloy electrode was evaluated by a linear polarization method. The diffusion coefficient D of hydrogen in the bulk of the alloys was examined by the potential-step method. The experimental details have been reported previously [5].

3. Results and discussion

3.1. Crystal structures

Fig. 1 shows the XRD patterns of La$_2$Mg(Ni$_{1-x}$Al$_x$)$_9$ alloys. It is found that all the alloy samples contain a main phase with hexagonal PuNi$_3$ type structure and a small quantity of the impurity phase (La$_2$Ni$_7$), which probably resulted from the incomplete reaction during sintering. Table 1 shows the lattice parameters and unit cell volumes of the alloys. It
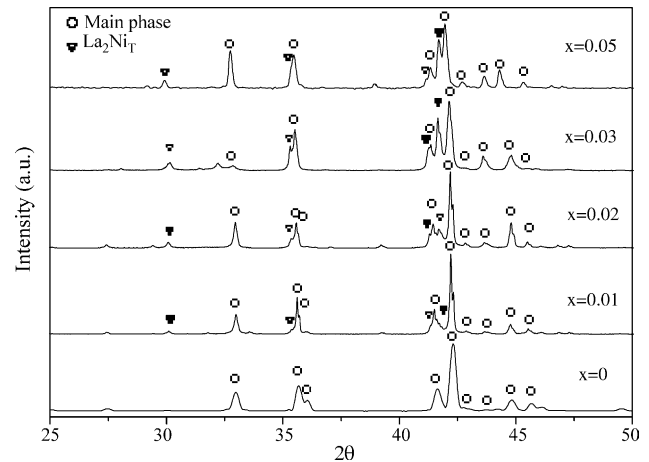

Fig. 1. XRD patterns of La$_2$Mg(Ni$_{1-x}$Al$_x$)$_9$ ($x = 0$–0.05) alloys.

can be seen that the progressively increased substitution of Al for Ni in the alloys leads to an increase of both a parameter (+0.89%) and c parameter (+1.4%), and a subsequent expansion of the unit cell volume (+3.2%) owing to the larger atomic radius of Al (1.82 Å) than that of Ni (1.62 Å). From the XRD patterns of the hydrides of La$_2$Mg(Ni$_{1-x}$Al$_x$)$_9$ ($x = 0$–0.05) alloys, it is found that the hydrides still preserve the hexagonal PuNi$_3$-type structure. The unit cell dimensions for these hydrides are also listed in Table 1. It can be seen that in the composition range of $x = 0$–0.03, the increase of x leads to an obvious decrease in the value of $\Delta V/V$ (from 24.8 to 21.4%), while the value of $\Delta V/V$ increases to 23.4% at $x = 0.05$. The result reveals that the unit cell volume expansion induced by hydrogenation can be largely reduced by a proper substitution of Ni with Al in the alloys.

3.2. Thermodynamic characteristics

The electrochemical P–C desorption isotherms measured at 25 °C in the La$_2$Mg(Ni$_{1-x}$Al$_x$)$_9$–H system are shown in Fig. 2. It can be seen that the desorption plateau pressure reduces noticeably as the Al content of the alloys increases, decreasing from 0.093 atm ($x = 0$) to 0.041 atm at $x = 0.03$. However, the slope of the desorption curve for the hydride with $x = 0.05$ becomes very steep with no clear plateau and a big portion of hydrogen absorbed remained undesorbed at $P_{eq} = 0.001$ atm. We believe that this feature and

Table 1
Lattice parameters of La$_2$Mg(Ni$_{1-x}$Al$_x$)$_9$ alloys and La$_2$Mg(Ni$_{1-x}$Al$_x$)$_9$H$_y$ hydrides

x	Alloys				Hydrides				$\Delta V/V$(%)
	a (Å)	c (Å)	V (Å^3)	c/a	a (Å)	c (Å)	V (Å^3)	c/a	
0	5.0336	24.2759	532.7	4.82	5.3809	26.5379	665.4	4.93	24.8
0.01	5.0503	24.3072	536.9	4.81	5.3801	26.3057	659.4	4.89	22.8
0.02	5.0537	24.3160	537.8	4.81	5.3725	26.1489	653.7	4.87	21.6
0.03	5.0579	24.3257	538.9	4.81	5.3795	26.1145	654.5	4.85	21.4
0.05	5.0783	24.6198	549.9	4.85	5.3180	27.7038	678.5	5.21	23.4

Table 2
The electrochemical properties of the La$_2$Mg(Ni$_{1-x}$Al$_x$)$_9$ ($x = 0$–0.05) alloys

x	H/M	C_{max} (mAh/g)	N_a[a]	HRD$_{800}$ (%)	I_0 (mA/g)	$D (\times 10^{-10}$ cm^2 s^{-1})	V_H[b] (Å^3/H atom)	S_{150} (%)
0	1.03	400.2	2	72.8	88.5	7.10	3.61	57.9
0.01	1.01	385.8	3	24.1	65.4	3.90	3.37	68.8
0.02	0.987	374.5	3	13.8	62.8	3.63	3.22	73.8
0.03	0.925	353.1	3	28.3	66.7	3.13	3.57	60.3
0.05	0.889	221.5	5	33.6	75.6	1.18	3.89	63.5

[a] The cycle numbers needed to activate the electrodes.

[b] The volume expansion of the unit cell per H atom absorbed which is calculated according to Ref. [6].
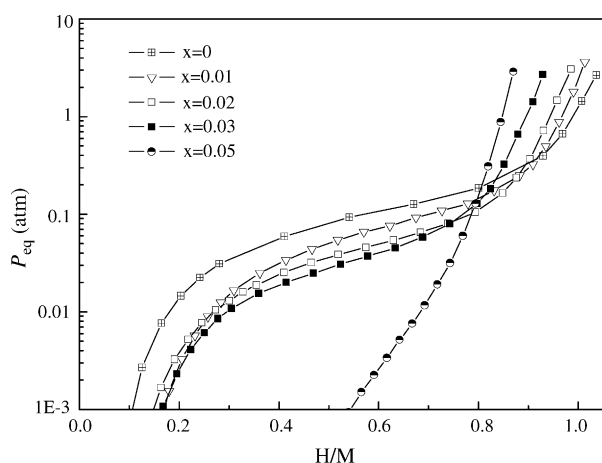

Fig. 2. The electrochemical desorption *P–C* isotherms for La$_2$Mg(Ni$_{1-x}$Al$_x$)$_9$ ($x = 0$–0.05) alloys at 25 °C.

the observed broadening peaks in the XRD pattern of this alloy hydride reveal that a certain portion of the crystalline alloy with $x = 0.05$ has been changed to the amorphous state upon hydriding.

As also shown in Table 2, the hydrogen storage capacity (H/M) of the alloys decreases from 1.03 to 0.889 when the Al content increases from $x = 0$ to 0.05. This is believed attributable to the high stability of the hydrides of the Al-substituted alloy, being too stable to desorb hydrogen readily during testing.

3.3. Electrochemical properties

The electrochemical properties of the tested alloys are listed in Table 2. It can be seen that all the alloys can be easily activated to reach their maximum capacity within 5 cycles. For the alloys with composition range of $x = 0$–0.03, the maximum discharge capacity (C_{max}) decreases slightly with the increase of x (from 400.2 to 353.1 mAh/g), and then decreases sharply to 221.5 mAh/g as $x = 0.05$. The variation of maximum discharge capacity of the alloys agrees basically with the variation of the H/M measured for alloys with different Al contents.

From Table 2, it can be seen that as the Al content increases, the HRD$_{800}$ of the alloys decreases sharply from 72.8% ($x = 0$) to 13.8% ($x = 0.02$), and then slightly increases to the range of 28.3–33.6% ($x = 0.03$–0.05). It is known that the high-rate dischargeability of a MH electrode is

mainly influenced by the electrochemical reaction kinetics on the alloy surface and the diffusion rate of hydrogen in the alloy bulk [9]. As shown in Table 2, the measured exchange current density I_0 of the alloy electrodes decreases from 88.5 mA/g ($x = 0$) to 62.8 mA/g ($x = 0.02$), and then increases to the range of 66.7–75.6 mA/g when x increases further. This indicated that the poor HRD$_{800}$ of the Al-substituted alloy electrodes is obviously related to their decreased electrocatalytic activity for the hydrogen electrode reaction. Also from Table 2, it can be seen that the diffusion coefficient (D) of hydrogen in the bulk of the alloys decreases with increasing Al content, which agrees with the increased hydride stability of the alloys. Therefore, it is believed that the lower hydrogen diffusion rate in the Al-substituted alloys is another cause for their poor high-rate dischargeability.

Fig. 3 shows the discharge capacity of the alloys as a function of cycle number. The capacity retention rate after 150 cycles, expressed as $S_{150} (\%) = C_{150}/C_{max} \times 100\%$ (where C_{150} is the discharge capacity at the 150th cycles), is also listed in Table 2. It can be seen that the S_{150} of the alloys with $x = 0$–0.02 increase greatly from 57.9% ($x = 0$) to a much higher value of 73.8% for the alloy with $x = 0.02$, while the S_{150} of the alloys with $x = 0.03$–0.05 drops to 60.3–63.5%. It is well known that the cycling capacity decay of a MH electrode is influenced mainly by two factors: the surface passivation due to the oxidation of active components to form oxides or hydroxides and the molar volume of hydrogen, V_H, in the hydride phase [7]. On this basis, the improvement of cycling stability for the Al substituted alloys can be attributed to the
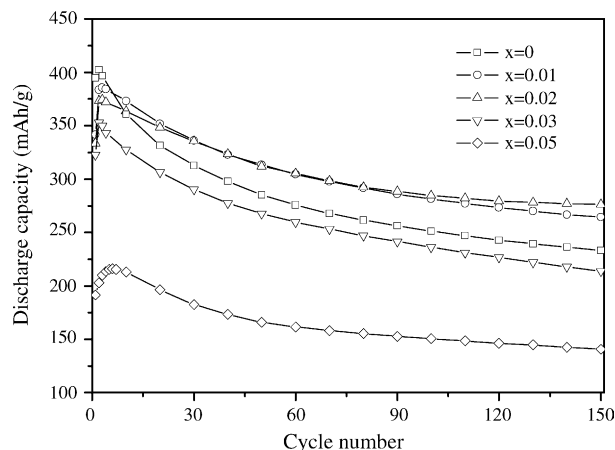

Fig. 3. Cycling stability of La$_2$Mg(Ni$_{1-x}$Al$_x$)$_9$ ($x = 0$–0.05) alloys at 25 °C.
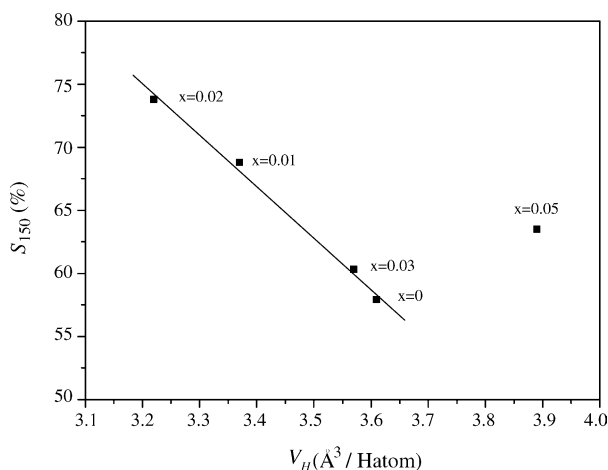
Fig. 4. Variation of the cycling capacity retention rate (S_{150}) with the molar volume of hydrogen (V_H) for $La_2Mg(Ni_{1-x}Al_x)_9$ ($x = 0$–0.05) alloys.

smaller V_H compared with that of the La_2MgNi_9 alloy (as shown in Table 2). The effect of Al content on the capacity retention rate (S_{150}) and the molar volume of hydrogen in the hydride phase (V_H) of the alloys are correlated and shown in Fig. 4. It can be seen that the value of S_{150} as a function of the value of V_H of the alloys with $x = 0$–0.03 shows a good linear relationship, indicating that the alloy with a smaller V_H results in an improved cycling stability. As to the alloy with $x = 0.05$, it shows a relatively higher S_{150} value than that of the alloy with $x = 0.03$ although its V_H value is even larger, its better cycling stability can probably be ascribed to the formation of part of amorphous hydride phase and the lower reversible hydrogen storage capacity of the alloy.

4. Conclusions

The effect of Al substitution for Ni on the structure and electrochemical properties of $La_2Mg(Ni_{1-x}Al_x)_9$ ($x = 0$–0.05) alloys has been investigated. It is found that the substitution does not change the main phase structure (the hexagonal $PuNi_3$-type structure) of the alloys. The increase

of Al content in the alloys leads to an increase in the cell volume and a noticeable decrease in cell volume expansion on hydriding and also leads to a higher hydride stability. With increasing Al content, the discharge capacity of the alloys at 50 mA/g slightly decreases from 400.2 mAh/g ($x = 0$) to 374.5 mAh/g ($x = 0.02$) and then sharply drops to 221.5 mAh/g at $x = 0.05$. As the Al content increases, the high-rate dischargeability (HRD_{800}) of the alloys decreases from 72.8% ($x = 0$) to 36.5% at $x = 0.05$. The decrease of HRD_{800} of the alloys is mainly attributed to the decrease of their electrocatalytic activity for the hydrogen electrode reaction and the lower hydrogen diffusion rate in the bulk of alloy. In the composition range of $x = 0$–0.02, the cycling stability (S_{150}) of the alloys improves greatly with increasing of x, increasing from 57.9% ($x = 0$) to 73.8% ($x = 0.02$), and then drops to the range of 60.3–63.5% when $x = 0.03$–0.05. The improvement in cycling stability is mainly attributed to the lower V_H in hydride phase.

References

[1] K. Kadir, N. Nuriyama, T. Sakai, I. Uehara, L. Eriksson, J. Alloys Comp. 284 (1999) 145.
[2] J. Chen, N. Kuriyama, H.T. Takeshita, H. Tanaka, T. Sakai, M. Haruta, Electrochem. Solid-State Lett. 3 (6) (2000) 249.
[3] T. Kohno, H. Yoshida, F. Kawashima, T. Inaba, I. Sakai, M. Yamamoto, M. Kanda, J. Alloys Comp. 311 (2000) 5.
[4] B. Liao, Y.Q. Lei, G.L. Lu, et al., J. Alloys Comp. 356/357 (2003) 746.
[5] B. Liao, Y.Q. Lei, L.X. Chen, et al., J. Power Sources 129 (2004) 358.
[6] J.J.G. Willems, Philips J. Res. Suppl. 39 (1984) 1.
[7] J.J.G. Reilly, J.O. Besenhard (Eds.), Metal Hydrides Electrodes, Handbook of Battery Materials, Wiley, New York, 2000.
[8] B. Liao, Y.Q. Lei, L.X. Chen, et al., J. Alloys Comp. 376 (2004) 186.
[9] C. Iwakura, M. Matsuoka, K. Asai, T. Kohno, J. Power Source 38 (1992) 335.